Nanoscale

Continuous Production of Nitrogen-Functionalized Graphene Nanosheets for Catalysis Applications

Journal:	*Nanoscale*
Manuscript ID:	NR-ART-05-2014-002824.R2
Article Type:	Paper
Date Submitted by the Author:	07-Aug-2014
Complete List of Authors:	Sanjeeva Rao, Kodepelly; National Cheng Kung University, PCGMR,MS & E Senthilnathan, Jaganathan; National Cheng Kung University, PCGMR,MS & E Ting, Jyh-Ming; National Cheng Kung University, MS & E Yoshimura, Masahiro; National Cheng Kung University, PCGMR,MS&E; National Cheng Kung University, PCGMR,MS & E

Continuous Production of Nitrogen-Functionalized Graphene Nanosheets for Catalysis Applications

Kodepelly Sanjeeva Rao, Jaganathan Senthilnathan, Jyh-Ming Ting, Masahiro Yoshimura*

Promotion Center for Global Materials Research (PCGMR), Department of Material Science and Engineering, National Cheng Kung University, Tainan, Taiwan

*Corresponding author. Tel.: +886-6-2757575 ext. 62013; Fax: +886-6-2760112;
E-mail: yoshimur@mail.ncku.edu.tw (Masahiro Yoshimura)

This study reports the “continuous production” of high-quality, few-layer nitrogen-functionalized graphene nanosheets in aqueous solutions directly from graphite via a two-step method. The initial step utilizes our recently developed peroxide-mediated soft and green electrochemical exfoliation approach for the production of few-layer graphene nanosheets. The subsequent step, developed here, produces nitrogen-functionalized graphene nanosheets via selective alkylation/basic hydrolysis reactions using rather a simple nitrogen precursor bromoacetonitrile, which is never reported in the literature. A possible reaction mechanism of the nitrogen-functionalized graphene formation is proposed. The proposed method allows the quantification of the phenolic and hydroxyl functional groups of anodic few-layer graphene via the derivatization chemistry approach. Additionally, a nitrogen-functionalized graphene-gold nanocrystals hybrid is prepared using gold nanocrystals obtained via the microwave irradiation of $H[AuCl_4]$ and trisodium citrate solution. A systematic investigation demonstrates that the nitrogen-functionalized graphene-gold nanocrystal hybrid shows enhanced catalytic reduction of carbonyl compounds such as benzaldehyde.

Keywords: Graphene, synthesis, soft processing, derivatization chemistry, catalysis

Introduction

Graphene, a two-dimentional π-networked nanomaterial, is a candidate for future nanoelectronics due to its atomic thickness and excellent properties.[1-4] The development of synthetic methods for the preparation[5-9] of graphene-based materials has received a lot of interest due to the potential applications of such materials in various fields, including energy storage, electronics, sensors, catalysis, and biomedical applications. Graphene must be prepared with a specific morphology by controlled methods to investigate its practical applications. In addition to the morphological manipulation of graphene, chemical functionalization is an efficient approach for tailoring graphene properties. Resultantly, the properties of nitrogen-functionalized graphene (N-FG)[10-18] were found to be superior to those of pristine graphene. For example, edge-functionalized N-FG behaves as an electron-rich n-type field-effect transistor.[16] N-FG can work as a metal-free catalyst[11] with enhanced properties for the oxygen reduction reaction in alkaline fuel cells. N-FG is also useful for semiconductor devices, batteries, sensors, and ultracapacitors. Therefore, numerous preparation methods of N-FG have been developed, such as those based on annealing, arc discharge, chemical vapor deposition, and solution processing.[10-15] Among solution processing,[5-8, 19-22] electrochemical exfoliation methods[23-24] have been found to be efficient and environmentally friendly. However, electrochemical approaches generally produce unfunctionalized or ionic-liquid-functionalized graphene materials.

Methods for the nitrogen functionalization of graphene materials often utilize filtration and/or drying of the products or high-temperature treatment in a multi-step procedure. For example multi-stage, high temperature pyrolysis methods[17-18] with high quantity of nitrogen precursors could form products having higher nitrogen

contents (2.04% to 19.46%). Although, the preparation of functionalized graphene by even three-step electrochemical approaches is rare,[25] the present study could develop an efficient method for the "continuous production" of N-FG nanosheets directly from graphite via a two-step method. The initial step utilizes our recently developed electrochemical soft processing approach,[23] where high-quality, anodic few-layer graphene (AFLG, product I) nanosheets in aqueous solution were formed. The subsequent second step, developed here, directly utilizes the AFLG aqueous dispersion formed in the previous step for nitrogen functionalization, which leads to the formation N-FG (product II). Thus a simple but versatile approach has been proposed for "continuous production" of N-FG nanosheets directly from graphite without any additional multiple processing such as filtration, drying or firing processes, which is exactly our project target. The proposed nitrogen functionalization improves the dispersibility of N-FG in various solvents and introduces active nitrogen centers, which is important in various applications. In order to demonstrate these merits, N-FG and gold nanocrystals (AuNCs) were used for the preparation of an N-FG-AuNCs hybrid (product III). The obtained N-FG and AuNCs are characterized using various techniques. The quantification of the phenolic and hydroxyl groups of AFLG is conducted based on the derivatization chemistry approach. The catalytic efficiency of the N-FG-AuNCs hybrid for the reduction of benzaldehyde is also evaluated.

Experimental section

Chemicals: Trisodium citrate dihydrate (TSC) with 99% purity was purchased from Riedel-deHaen, Germany. Hydrogen tetrachloroaurate-(III) trihydrate ($HAuCl_4 \cdot 3H_2O$) with 99.99% metal basis purity and high-purity (99.9995%) graphite rods, 6.15 mm in diameter and 152 mm in length, were obtained from Alfa Aesar. Other chemicals

were received from Sigma-Aldrich and used without additional purification. All solvents used in this study were of HPLC grade. A Roda purification system (Te Chen Co. Ltd, Taiwan) was used for the purification of aqueous solutions with Milli-Q water (> 18.2 MΩ).

Preparation of N-FG:

In the first step, 90 mg of AFLG[23] nanosheets were formed in an aqueous solution via electrochemical exfoliation of graphite using simply aqueous 3.0 M NaOH solution (75 ml) with 130 mM H_2O_2, and a working bias voltage of 1 V for 10 min and 3 V for 10 min at room temperature. The as prepared AFLG nanosheets in an aqueous solution with pH 11.8 were directly subjected to nitrogen functionalization (second step) without any filtration, drying or firing processes. Therefore we have described the present method as "continuous production of N-FG" even it uses two steps in solutions. The AFLG nanosheets in aqueous solution were directly treated with aqueous 6.0 M HCl solution (33 ml) at 0 °C. A solution of bromoacetonitrile (0.1 ml, weight ratio of AFLG/$BrCH_2CN$ = 1/2) in dioxane (5 ml, H_2O:dioxane = 22:1) was added to the resulting reaction mixture, which was then degassed using nitrogen gas bubbling. The reaction mixture was sonicated at room temperature for 30 min and then refluxed at 100 °C for 10 min. The reaction mixture was cooled to room temperature and neutralized with 6.0 M HCl solution (2 ml). The reaction mixture was filtered with 100-nm porous filters, washed with excess deionized water by vacuum filtration, and then dried in an oven for 2 h at 60 °C. The obtained dry powders (105 mg) were dispersed into appropriate solvents by gentle water-bath ultrasonication for 5 min. The resulting N-FG in acetonitrile (ACN) was additionally diluted with excess water. The obtained supernatant dispersions were used for further characterizations.

Preparation of citrate-stabilized AuNCs: Citrate-stabilized AuNCs were prepared

using the following method. The reaction was performed in a microwave reactor (Scientech, Taiwan). In a typical procedure, aqueous TSC (9 ml, 0.03 M) was added to an aqueous $H[AuCl_4]\cdot 3H_2O$ solution (30 ml, 0.5 mM), which was then subjected to microwaves (90 W) at 120 °C for 3 min. The resulting light pink aqueous dispersion was centrifuged at 8000 rpm and washed with Milli-Q water. The supernatant aqueous dispersion of citrate-stabilized AuNCs was directly used for further applications.

Preparation of N-FG-AuNCs hybrid: N-FG aqueous dispersion (15 ml, 0.50 mg/ml) was mixed with 5.0 ml of citrate-stabilized AuNCs in aqueous solution (relative volume ratio of AuNCs to N-FG = 0.33). The reaction mixture was sonicated at room temperature for 30 min and washed with Milli-Q water. The same procedure was used for the preparation of AFLG-AuNCs hybrid. The resulting aqueous dispersions were directly used for further applications.

Catalytic Reduction of Benzaldehyde: An aqueous solution of N-FG-AuNCs hybrid (0.50 mol% with respect to gold concentration) was added to 10 ml of an aqueous benzaldehyde solution (7.50×10^{-4} M) with stirring. Then, 1.0 ml of an aqueous 2.22 X 10^{-2} M $NaBH_4$ solution (3 equiv. with respect to benzaldehyde) was added drop-wise and stirred continuously at room temperature for an appropriate time. The reaction progress was monitored using ultraviolet-visible (UV-vis) spectroscopy. The samples for UV-vis spectroscopy were prepared by collecting a small quantity of the reaction mixture at regular time intervals. The same procedure was used for the reduction of benzaldehyde in the presence of AFLG-AuNCs hybrid, N-FG, and AuNCs.

Characterizations

High-resolution transmission electron microscopy (HR-TEM; JOEL, JSM 2100F) analysis was used to investigate the nanostructure and surface morphology of N-FG

and AuNCs at an acceleration voltage of 200 kV. An energy-dispersive X-ray spectroscopy (EDS) detector attached to the transmission electron microscope was utilized for the compositional analysis of AuNCs. The carbon, oxygen, and nitrogen binding energies of graphite and N-FG were evaluated using X-ray photoelectron spectroscopy (XPS) measurements (ULVAC Inc., PHI Quantera SXM). A confocal micro-Raman spectrometer (Renishaw inVia) was used to evaluate the Raman spectra of graphite and N-FG with an argon ion laser at a 633 nm excitation wavelength. The wavenumber was calibrated using the Si peak at 520 cm^{-1} as a reference. Fourier transform infrared (FT-IR) spectroscopy (Vertex 70, Bruker, Germany) was used for recording spectra in a range of 400 to 4000 cm^{-1}. Optical absorption spectra of AuNCs and the reduction reaction kinetics were measured using a UV-vis spectrophotometer (JASCO V-670). TEM samples were obtained by drop-casting redispersed solutions onto carbon-coated Cu grids and evaporating them at 60 °C for 30 min. Raman spectroscopy and XPS samples were obtained by the deposition of redispersed materials on a glass substrate and evaporating them at 60 °C for 30 min. The KBr disc method was used for the preparation of FT-IR samples. The samples for UV-vis spectral measurements were prepared by adding an equal volume of Milli-Q water to all samples.

Results and discussion

Formation of N-FG

A schematic illustration of the experimental process for the preparation of N-FG is presented in Figure 1a. In the first step, our recently developed[23] electrochemical strategy is applied for formation of high-quality, AFLG nanosheets in aqueous solution and was further reacted with HCl. This HCl-treated AFLG was reacted[26] with

bromoacetonitrile over 30 min sonication at room temperature and subsequent reflux[27] for 10 min to produce N-FG. Photographs of exfoliated AFLG (Figure 1a, product I) and N-FG (Figure 1a, product II) nanosheets directly in electrolyte are shown. The purified N-FG nanosheets were redispersed in dimethyl formamide (DMF), ethylene glycol (EG), tetrahydrofuran (THF), and ACN, respectively, and were stable for over a month (Figure 1b). Figure 1c shows N-FG nanosheets redispersed in ACN after additional dilution (see experimental section).

A schematic of the size-controlled synthesis of AuNCs is presented in Figure 1d. An aqueous mixture of 0.40 mM $H[AuCl_4]$ and 0.03 M TSC was subjected to microwave irradiation at 120 °C for 3 min, forming AuNCs with a size of 4-12 nm (Figure S1, Supporting Information (SI)). Figure 1e shows the preparation method of AFLG-AuNCs hybrid (product III) and N-FG-AuNCs hybrid (product IV) under sonication for 30 min. The nitrogen groups of N-FG make it well dispersible in aqueous solution but AFLG nanosheets are not dispersible. The AuNCs are also well dispersible. Therefore, the N-FG nanosheets, but not AFLG nanosheets, were decorated with AuNCs in the aqueous solution. The as-prepared N-FG and AuNCs were characterized using various techniques.

Structural features of N-FG

Raman spectroscopy is a powerful, noninvasive technique for characterizing carbon nanomaterials, especially for measuring defects and ordered/disordered carbon structure.[28-29] It was thus applied to study the structural features of graphite and N-FG (Figure 2). The Raman spectrum of graphite (Figure 2a) show a D band and a small D' shoulder band at 1337 and 1621 cm^{-1}, respectively. The G band and intense 2D

band are located at 1581 and 2664 cm^{-1}, respectively. The Raman spectrum of N-FG (Figure 2b) shows a D band related to the disorder mode at 1339 cm^{-1} and a D' shoulder band corresponding to the disorder of edge carbons at 1616 cm^{-1}. The G band corresponding to ordered in-plane sp^2 carbon atoms at 1579 cm^{-1} is a doubly degenerate (TO and LO) phonon mode (E_{2g} symmetry). The symmetric intense 2D band at 2667 cm^{-1} originates from two-phonon double resonance, indicating the presence of few-layer graphene.[30] The ratio of the integrated intensities of the D and G modes (I_D/I_G) of N-FG is (0.73) is higher than that of graphite (0.54). The Raman results of N-FG are in good agreement with results reported in our recent report.[31]

The HR-TEM results confirm the structure of N-FG (Figure 3). A low-magnification HR-TEM image of an N-FG nanosheet on a carbon grid shows that the material consists of randomly aggregated interconnected thin sheets (Figure 3a). The selected-area image reveals low-defect/defect-free domains of N-FG nanosheets (Figure 3b). The HR-TEM images of N-FG show the existence of large defect-free sp^2-network domains (Figure 3c), crystalline edges (Figures 3e), and few-layer graphene with a lattice spacing of 0.35 nm (Figure 3f). The electron diffraction patterns of the carbon lattice show the presence of a low-defect sp^2 network (Figure 3d). The observed lattice spacing of N-FG nanosheets is in good agreement with values reported in the literature.[31]

The XPS results reveal the nature of oxygen and nitrogen functional groups and the level of oxygen/nitrogen insertion into N-FG during the continuous preparation process (Figure 4). Nitrogen was detected in the wide-scan XPS spectrum of N-FG, as well as carbon and oxygen, whereas only carbon and oxygen were detected for

graphite (Figure 4a). The starting graphite has a carbon-to-oxygen ratio (C/O) of 98.5:1.5, and N-FG has a carbon-to-oxygen-to-nitrogen ratio (C/O/N) of 92.5:4.6:2.9. Thus, during the second step of N-FG formation, nitrogen functional groups were inserted. This explains the observed enhanced dispersibility and stability of N-FG in various solvents (Figure 1b). The nitrogen functional groups present in N-FG facilitate its dispersion in various solvents. Only 5 min of sonication is enough for N-FG dispersion, whereas 10 min is needed for AFLG[23] dispersion. The analysis of numerically fitted C1s core levels of graphite (Figure 4b) and N-FG (Figure 4c) indicates that both samples were asymmetric and thus both samples contained functional groups.

The bands corresponding to the graphitic carbon bonds (C-C) of graphite and N-FG are identical (located at 284.8 eV) and the bands corresponding to C-OH bonds vary slightly (located at 285.9 and 285.4 eV for graphite and N-FG, respectively). Additionally, a new peak at 286.9 eV, corresponding to the C-O (alkoxy) group, appears in the N-FG XPS spectrum. The bands corresponding to C-N bonds appear at the same position (285.4 eV) as bands corresponding to C-OH bonds. N-FG contains peaks at 284.8, 285.4, and 286.9 eV, corresponding to C-C, C-OH/C-N, and C-O groups, respectively, which are in good agreement with the bands in NFG prepared by chemical vapor deposition.[32-34] The N1s XPS spectrum of N-FG shows a broad peak at 399.8 eV corresponding to the HN-C=O group and a peak at 401.6 eV attributed to NH_2 groups (Figure 4d).[35-37] These results confirm the insertion of nitrogen functional groups into N-FG during the second step of its formation. The highly graphene nature of N-FG also confirmed by these results because it has graphene sheets with low content of oxygen unlike graphene oxide or even graphene in some cases.[6]

The insertions of oxygen and nitrogen functional groups into N-FG were further confirmed by FT-IR spectroscopy (Figure 5). The FT-IR spectra of graphite (Figure 5a) and N-FG (Figure 5b) contain peaks at around 1400 and 1000 cm^{-1}, corresponding to CO-H and C-O stretching modes, respectively, and a peak at 3345 cm^{-1}, corresponding to the CO-H bending mode related to the hydroxyl functional group.[38] The peaks corresponding to sp^2-network domains (C=C stretching) and the coupling of C-N stretching with N-H deformation vibration appear at 1588 cm^{-1}. Additionally, N-FG shows C-N and C=O stretching modes at around 1000 and 1623 cm^{-1}, respectively, and a peak at around 3350 cm^{-1}, corresponding to the N-H bending mode related to amide functionality.[39-40] The peaks corresponding to C-H (O-CH_2CONH_2) in-plane bending and stretching vibrations are appeared at 1025, 2775, cm^{-1} respectively.[6] These results confirm the insertion of nitrogen functional groups into N-FG during the second step of its formation. These FT-IR results are consistent with XPS results.

Chemistry of N-FG: Quantification of phenolic and hydroxyl groups of AFLG

Functionalization is a versatile method for tuning chemical and electronic properties via the modification of functional groups by synthetic organic chemistry. Thus, understanding the existing functional groups and their composition in materials is very important. Traditional analysis techniques generally cannot differentiate phenolic and hydroxyl groups. The derivatization chemistry[41-46] approach (which uses the formation of a derivative such as a functionalized material) is a commonly used method for the quantification of functional groups via selective (only one functional group reaction) and clean (complete conversion) derivatization and subsequent analysis. Traditional-organic-chemistry-based selective organic functionalization[47-52]

of graphene materials is also well established in the literature. An approach based on derivatization chemistry is used here for the quantification of the phenolic and hydroxyl groups of AFLG. The structural features and formation mechanism of N-FG (Figure 6) are proposed based on experimental results and published literature.[40] AFLG has two kinds of oxygen functional group, namely phenolic groups on sheet edges and hydroxyl groups on the basal plane.[23] Aqueous NaOH selectively and cleanly reacts with the phenolic groups[26] of AFLG. Subsequent selective nitrogen functionalization occurs to produce N-FG in the second step. The XPS spectrum of N-FG was used for the quantification of the phenolic and hydroxyl groups of AFLG.

The phenolic groups of AFLG exist in the form of sodium phenoxide via reaction[26] with sodium hydroxide, as shown in Figure 6. The hydroxyl groups of AFLG do not undergo a reaction with NaOH because they are relatively weakly acidic. Thus, treatment of AFLG with bromoacetonitrile at room temperature forms phenoxylated ACN selectively and the subsequent 10 min reflux converts nitrile (C≡N) groups into imidol groups via NaOH-mediated selective hydrolysis. Over reaction time cause to loss of nitrogen from N-FG as NH_3 gas. These hydrolysis trends of nitrile compounds are quite common in organic chemistry.[53] The hydrolysis mechanism involves an attack by hydroxide anions on the carbon center of the C≡N group and subsequent proton addition to the nitrogen center leads to the formation of imidol.[54] The imidol undergoes tautomerism[54] via rapid intra-molecular migration of a proton to form phenoxylated amides bearing N-FG. Thus, it can be concluded that only phenolic groups selectively undergo nitrogen functionalization. Therefore, it is proposed that AFLG contains around 2.9% phenolic groups and 2.6% hydroxyl groups of the total 5.5% oxygen functional groups because 2.9% nitrogen was inserted during the second step of N-FG formation (Figure 7). Even though our present method produces N-FG

with only 2.9% nitrogen content, it is a most effective method as it is a simple but versatile "solution processing" approach unlike high temperature pyrolysis reported in the literature.[17-18] The XPS analysis show that the removal of hydroxyl groups and insertion of nitrogen functional groups occurred during the second step of N-FG formation. The quantity of oxygen functional groups in N-FG is thus lower than that in AFLG. The NaOH-induced removal of hydroxyl groups of AFLG is supported by the literature[55] and is an additional benefit of our method. The quantified phenolic and hydroxyl groups of AFLG are also useful for the design and controlled synthesis of new graphene-based materials. Thus, the proposed method has high potential for the preparation of various N-FG-based materials by using modified molecules of Br-CH_2-CN (Br = Br, Cl, I, -OTs and CN = pyrrole, piperidine, NH_2, proline, thiophene moieties) as nitrogen precursors. In this case, only alkylation is enough but no hydrolysis required as they do not possess nitrile groups.

N-FG-AuNCs hybrid formation

The AFLG-AuNCs and N-FG-AuNCs hybrids were prepared using purified AFLG, N-FG, and AuNCs under sonication. The size-controlled AuNCs were obtained via the TSC-assisted reduction of H[$AuCl_4$] precursor under microwave irradiation (Figure S1, SI). The AFLG-AuNCs and N-FG-AuNCs hybrids were applied for the reduction catalysis of benzaldehyde.

Reduction Catalysis

The synthesis of alcohols via the reduction of carbonyl compounds is one of the most widely used reactions in organic chemistry.[56] Several carbonyl reduction methods[56] have been developed. However, they have several disadvantages, including the use of

toxic chemicals, complex procedures, and sensitive conditions, and long reaction times. We report herein the reduction of a carbonyl compound, benzaldehyde, using an $NaBH_4/H_2O$ system in the presence of N-FG-AuNCs and AFLG-AuNCs hybrids, N-FG, AuNCs (Figure 8). The low cost, environmental friendliness and easy operation of the $NaBH_4/H_2O$ system make it popular for the reduction of nitroarenes[57-58] catalyzed by carbon-based gold nanocrystal hybrids.

Time-resolved UV-vis spectroscopy was used to monitor the reaction progress. The UV-vis spectra of benzaldehyde show bands at 243 and 285 nm, corresponding to C=C and C=O, respectively.[59] As the reaction proceeded, the intensity of these bands decreased and finally disappeared and a new band appeared at 259 nm, corresponding to the C=C bonds of benzyl alcohol. The UV-vis spectra show that the required reaction time of N-FG-AuNCs hybrid is only 3 min, whereas those of AFLG-AuNCs hybrid, AuNCs, and N-FG are 12, 20, and 40 min, respectively. The catalysis results prove that AuNCs (Figure 8a) and N-FG (Figure 8b) are catalytically inactive, and that N-FG-AuNCs hybrid (Figure 8c) is catalytically superior to AFLG-AuNCs hybrid (Figure 8d). The observed catalytic reaction trends are described by considering two factors, namely dispersibility and adsorption. N-FG-AuNCs hybrid (Figure 1e, product IV), but not AFLG-AuNCs hybrid (Figure 1e, product III), had good dispersibility in the reaction medium (aqueous solution). Therefore, the N-FG nanosheets, but not AFLG nanosheets, were decorated with AuNCs. The efficient adsorption of benzaldehyde onto N-FG/AFLG nanosheets is very important for effective catalysis reaction. Nitrogen groups are basic in nature and they have strong affinity towards acidic molecules[60] or even partially electron-polarizable molecules such as benzaldehyde. Thus, the nitrogen groups of N-FG facilitate the efficient adsorption of benzaldehyde and the subsequent reaction is catalyzed by AuNCs. The

efficient adsorption and good dispersibility of N-FG in aqueous solution and AuNCs catalysis makes the N-FG-AuNCs hybrid a superior catalytic system over the AFLG-AuNCs hybrid, which lacks nitrogen groups and does not make AuNCs available for catalysis. The proposed mechanism of benzaldehyde adsorption on N-FG nanosheets and subsequent AuNCs-mediated reduction catalysis is consistent with a literature report[58] on nitroarene reduction catalyzed by a graphene oxide-AuNCs hybrid. The present study reports the high catalytic efficiency of the N-FG-AuNCs hybrid for benzaldehyde reduction in the first time. Therefore high-quality N-FG nanosheets with low level damage were obtained using the proposed two-step solution processing approach under mild conditions. As N-FG possess sterocenters, its AuNCs hybrid is useful for stereoselective reduction of benzaldehyde in presence of other functional groups because functional groups with different chemical environment show different reactivity. The reduction catalysis product benzyl alcohol is an important core moiety in several bioactive molecules[61-63] such as goniotriol and goniofufurone anti-tumor agents (Figure 8e).

The comparative study[57-58, 64-66] of preparation and catalysis trends of carbon material-gold nanocomposites is presented (Table 1). The present method has several advantages such as (a) easy (continuous) production of N-FG unlike using complex procedure and/or high temperature treatment and/or, multi-stage reactions and/or high reaction time and/or toxic chemicals and/or filtration, drying of products at each stage in a multi-step reaction (entries 1-5), (b) possible production of various N-FG-based materials, (c) good dispersibility of our N-FG in various solvents, (d) good catalytic efficiency of our N-FG-AuNCs hybrid (only 3 min reaction time and 3 equivalents of $NaBH_4$) unlike high reaction time (15-140 min, entries 1, 3, 4) and 100-350 equivalents of $NaBH_4$ (entries 2-5). All these merits make our simple but versatile

"continuous production" approach as novel and efficient method.

Conclusion

This study developed a simple but versatile approach for the "continuous production" of high-quality, few-layer N-FG nanosheets directly from graphite via electrochemical exfoliation and subsequent selective nitrogen functionalization using a simple bromoacetonitrile precursor via alkylation/basic hydrolysis as the key steps. The proposed formation mechanism of N-FG reveals that the preformed phenoxide ions of AFLG react with bromoacetonitrile and that subsequent selective basic hydrolysis converts nitrile into the amide group. The stable dispersions of N-FG nanosheets in DMF, EG, THF, and ACN could be useful in several applications, such as catalysis. The NaOH-induced removal of hydroxyl groups of AFLG during the second step of N-FG formation is an additional benefit. The proposed method makes the mass production of N-FG possible. The derivatization-chemistry-based quantification approach indicates the presence of 2.9% phenolic and 2.6% hydroxyl groups in AFLG. Additionally, N-FG-AuNCs hybrid was prepared using citrate-stabilized AuNCs 4-12 nm in size. The N-FG-AuNCs hybrid proved to be an efficient catalyst for benzaldehyde reduction and the produced benzyl alcohol is a core moiety of several bioactive molecules. The simplicity of the developed method and the high performance of produced products make the proposed approach suitable for the production of various N-FG-based materials.

Acknowledgements

The authors would like to thank professors Jiunn-Der Liao, Jih-Jen Wu, and Mario Hofmann and Dr. Wan-Hsiun Lin, Ms. Pei-Ru So, and Mr. Hsun-Wei Cho for their

help in this research. This research project was supported by National Cheng Kung University, Taiwan.

References

1. M. I. Katsnelson, K. S. Novoselov and A. K. Geim, *Nat. Phys*., 2006, **2**, 620-625.
2. K. S. Novoselov, Z. Jiang, Y. Zhang, S. V. Morozov, H. L. Stormer, U. Zeitler, J. C. Maan, G. S. Boebinger, P. Kim and A. K. Geim, *Science*, 2007, **315**, 1379.
3. F. Wang, Y. Zhang, C. Tian, C. Girit, A. Zettl, M. Crommie and Y. R. Shen, *Science*, 2008, **320**, 206-209.
4. C. Lee, X. D. Wei, J. W. Kysar and J. Hone, *Science*, 2008, **321**, 385-388.
5. S. Park and R. S. Ruoff, *Nat. Nanotechnol.*, 2009, **4**, 217-224.
6. J. Senthilnathan, Y-F. Liu, K. Sanjeeva Rao and M. Yoshimura, *Sci. Rep.*, 2014, **4**, 4395-4401.
7. K. S. Novoselov, V. I. Fal′ko, L. Colombo, P. R. Gellert, M. G. Schwab and K. Kim, *Nature*, 2012, **490**, 192-200.
8. F. Bonaccorso, A. Lombardo, T. Hasan, Z. Sun, L.Colombo and A. C. Ferrari, *Mater. Today*, 2012, **15**, 564-589.
9. C. Zhu and S. Dong, *Nanoscale*, 2013, **5**, 1753-1767.
10. D. Yu, L. Wei, W. Jiang, H. Wang, B. Sun, Q. Zhang, K. Goh, R. Si and Y. Chen, *Nanoscale*, 2013, **5**, 3457-3464.
11. S. Guo and S. Dong, *Chem. Soc. Rev.*, 2011, **40**, 2644-2672.
12. Z-L. Wang, J-M. Yan, Y-F. Zhang, Y. Ping, H-L. Wang and Q. Jiang, *Nanoscale*, 2014, **6**, 3073-3077.
13. D. R. Dreyer, S. Park, C. W. Bielawski and R. S. Ruoff, *Chem. Soc. Rev.*, 2010, **39**, 228-240.

14. Q. Tang, Z. Zhou and Z. Chen, *Nanoscale*, 2013, **5**, 4541-4583.

15. H. Liu, Y. Liu and D. Zhu, *J. Mater. Chem.*, 2011, **21**, 3335-3345.

16. X. Wang, X. Li, L. Zhang, Y. Yoon, P. K. Weber, H. Wang, J. Guo and H. Dai, *Science*, 2009, **324**, 768-771.

17. K. Parvez, S. Yang, Y. Hernandez, A. Winter, A. Turchanin, X. Feng and K. Mu¨llen, *ACS Nano*, 2012, **11**, 9541-9550.

18. L-L. Tian, X-Y. Wei, Q-C. Zhuang, C-H. Jiang, C. Wu, G-Y. Ma, X. Zhao, Z-M. Zong and S-G. Sun, *Nanoscale*, 2014, **6**, 6075-6083.

19. H. Chang and H. Wu, *Energy Environ. Sci.*, 2013, **6**, 3483-3507.

20. M. Yoshimura, W. Suchanek and K-S. Han, *J. Mater. Chem.*, 1999, **9**, 77-82.

21. H. Hu, Z. Zhao, W. Wan, Y. Gogotsi and J. Qiu, *Adv. Mater.*, 2013, **25**, 2219-2223.

22. M. Yoshimura. *J. Mater. Sci.*, 2006, **41**, 1299-1306.

23. K. Sanjeeva Rao, J. Senthilnathan, Y-F. Liu and M. Yoshimura, *Sci. Rep.*, 2014, **4**, 4237-4242.

24. J. Liu, C. K. Poh, D. Zhan, L. Lai, S. H. Lim, L. Wang, X. Liu, N. G. Sahoo, C. Li, Z. Shen and J. Lin, *Nano Energy*, 2013, **2**, 377-386.

25. Y. L. Zhong and T. M. Swager, *J. Am. Chem. Soc.*, 2012, **134**, 17896-17899.

26. L. M. Hancock, L. C. Gilday, S. Carvalho, P. J. Costa, V. Flix, C. J. Serpell, N. L. Kilah and P. D. Beer, *Chem. Eur. J.*, 2010, **16**, 13082 -13094.

27. M. Gütschow and J. C. Powers, *J. Org. Chem.*, 2001, **66**, 4723-4727.

28. A. C. Ferrari and J. Robertson, *J. Phys. Rev. B*, 2000, **61**, 14095-14107.

29. L. G. Cancado, A. Jorio, E. H. M. Ferreira, F. Stavale, C. A. Achete, R. B. Capaz, M. V. O. Moutinho, A. Lombardo, T. S. Kulmala and A. C. Ferrari, *Nano Lett.*, 2011, **11**, 3190-3196.

30. A. C. Ferrari, J. C. Meyer, V. Scardaci, C. Casiraghi, M. Lazzeri, F. Mauri, S. Piscanec, D. Jiang, K. S. Novoselov, S. Roth and A. K. Geim, *Phys. Rev. Lett.*, 2006, **97**, 187401-187404.

31. J. Senthilnathan, K. Sanjeeva Rao and M. Yoshimura, *J. Mater. Chem. A*, 2014, **2**, 3332-3337.

32. D. Wei, Y. Liu, Y. Wang, H. Zhang, L. Huang and G. Yu, *Nano Lett.*, 2009, **9**, 1752-1758.

33. A. L. Mohana Reddy, A. Srivastava, S. R. Gowda, H. Gullapalli, M. Dubey and P. M. Ajayan, *ACS Nano*, 2010, **4**, 6337-6342.

34. Z. Luo, S. Lim, Z. Tian, J. Shang, L. Lai, B. MacDonald, C. Fu, Z. Shen, T. Yu and J. Lin, *J. Mater. Chem.*, 2011, **21**, 8038-8044.

35. A. J. Beck, J. D. Whittle, N. A. Bullett, P. Eves, S. M. Neil, S. L. McArthur and A. G. Shard, *Plasma Process. Polym.*, 2005, **2**, 641-649.

36. S. Rangan, F. Bournel, J. J. Gallet, S. Kubsky, K. L. Guen, G. Dufour and F. Rochet, *J. Phys. Chem. B*, 2005, **109**, 12899-12908.

37. M. J. Kim, Y. Jeong, S. Sohn, S. Y. Lee, Y. J. Kim, K. Lee, Y. H. Kahng and J. H. Jang, *AIP Adv.*, 2013, **3**, 012117.

38. L. Palombi, M. Feroci, M. Orsinia, L. Rossia and A. Inesi, *Tetrahedron Lett.*, 2002, **43**, 2881-2884.

39. Y. Liu, J. Zhou, X. Zhang, Z. Liu, X. Wan, J. Tian, T. Wang and Y. Chen, *Carbon*, 2009, **47**, 3113-3121.

40. V. Georgakilas, M. Otyepka, A. B. Bourlinos, V. Chandra, N. Kim, K. C. Kemp, P. Hobza, R. Zboril and K. S. Kim, *Chem. Rev.*, 2012, **112**, 6156-6214.

41. C. G. Daughlon, *EPA Environmental Sciences Division homepage*. The California Public Health Foundation 23 June 1988.
42. T. Gross, F. Pippig, B. Merz, R. Merz, U. Vohrer, R. Mix, H. Steffen, W. Bremser and W. E. S. Unger, *Plasma Process. Polym.*, 2010, **7**, 494-503.
43. S. Ershov, F. Khelifa, P. Dubois and R. Snyders, *ACS Appl. Mater. Interfaces*, 2013, **5**, 4216-4223.
44. N. Adden, L. J. Gamble, D. G. Castner, A. Hoffmann, G. Gross and H. Menzel, *Langmuir*, 2006, **22**, 8197-8204.
45. V. I. Povstugar, S. S. Mikhailova and A. A. Shakov, *J. Anal. Chem.*, 2000, **55**, 405-416.
46. M. Ostenson, H. Jarund, G. Toriz and P. Gatenholm, *Cellulose*, 2006, **13**,157-170.
47. M. Quintana, E. Vazquez and M. Prato, *Acc. Chem. Res.*, 2013, **46**, 138-148.
48. W. Ai, J-Q. Liu, Z-Z. Du, X-X. Liu, J-Z. Shang, M-D. Yi, L-H. Xie, J-J. Zhang, H-F. Lin, T. Yu and W. Huang, *RSC Adv.*, 2013, **3**, 45-49.
49. J. Park and M. Yan, *Acc. Chem. Res.*, 2013, **46**, 181-189.
50. Z. Jin, T. P. McNicholas, C-J. Shih, Q. H. Wang, G. L. C. Paulus, A. J. Hilmer, S. Shimizu and M. S. Strano, *Chem. Mater.*, 2011, **23**, 3362-3370.
51. L. Dai, *Acc. Chem. Res.*, 2013, **46**, 31-42.
52. J. H. Lee, S. Kang, J. Jaworski, K-Y. Kwon, M. L. Seo, J. Y. Lee and J. H. Jung, *Chem. Eur. J.*, 2012, **18**, 765-769.
53. J. K. Niemeier, R. R. Rothhaar, J. T. Vicenzi and J. A. Werner, *Org. Process Res. Dev.*, 2014, **18**, 410-416.
54. G-Q. Tang, J. MacInnis and M. Kasha, *J. Am. Chem. Soc.*, 1987, **109**, 2531-2533.
55. T. Kuila, P. Khanra, N. H. Kim, J. K. Lim and J. H. Lee, *J. Mater. Chem. A*, 2013,

1, 9294-9302.

56. L. Shi, Y. Liu, Q. Liu, B. Wei and G. Zhang, *Green Chem.,* 2012, **14**, 1372-1375.
57. H. Wang, Z. Dong and C. Na, *ACS Sustainable Chem. Eng.,* 2013, **1**, 746-752.
58. Y. Choi, H. S. Bae, E. Seo, S. Jang, K. H. Park and B-S. Kim, *J. Mater. Chem.,* 2011, **21**, 15431-15436.
59. M. Vilar and M. Navarro, *Electrochimica Acta,* 2010, **56**, 305-313.
60. M-C. Huang and H. Teng, *Carbon,* 2003, **41**, 951-957.
61. K. R. Prasad and S. L. Gholap, *J. Org. Chem.,* 2008, **73**, 2-11.
62. J. S. Yadav, B. M. Rao and K. Sanjeeva Rao, *Tetrahedron Asymmetry,* 2009, **20**, 1725-1730.
63. J. S. Yadav, B. M. Rao, K. Sanjeeva Rao and B.V. S. Reddy, *Synlett,* 2008, **7**, 1039-1041.
64. P. Roy, A. P. Periasamy, C-T Liang and H-T. Chang, *Environ. Sci. Technol.,* 2013, **47**, 6688-6695.
65. W. Wang, J. Gu, W. Hua, X. Jia and K. Xi, *Chem. Commun.,* 2014 (online).
66. J. Huang, L. Zhang, B. Chen, N. Ji, F. Chen, Y. Zhang and Z. Zhang, *Nanoscale*, 2010, **2**, 2733-2738.

Figure Captions

Figure 1. Preparation process of N-FG-AuNCs hybrid: (a) electrochemical experimental setup diagram (left); photographs of exfoliated AFLG (product I) and dispersed N-FG (product II) directly in reaction mixture; (b) photographs of stable dispersions of purified N-FG in various solvents; (c) photograph of diluted dispersion of N-FG nanosheets in ACN; (d) synthetic process of AuNCs; (e) preparation process of AFLG-AuNCs hybrid (product III) and N-FG-AuNCs hybrid (product IV).

Figure 2. Raman spectra of (a) graphite and (b) N-FG. The Raman spectra of N-FG reveal the presence of high-quality, few-layer graphene.

Figure 3. Structural investigation of N-FG by TEM analysis: (a) low-magnification TEM image of N-FG nanosheet suspended on carbon grid; (b) HR-TEM image of N-FG nanosheet; (c) corresponding selected-area image, which clearly shows presence of defect-free domains; (d) selected-area image of electron diffraction pattern corresponding to carbon lattice; (e) HR-TEM image of crystalline edges; and (f) HR-TEM image of tri-layer N-FG with lattice spacing of 0.35 nm.

Figure 4. XPS characterizations: (a) wide-range scanning XPS spectra of (i) graphite and (ii) N-FG, C1s XPS spectra of (b) graphite and (c) N-FG, and (d) N1s XPS spectrum of N-FG.

Figure 5. FT-IR spectra of (a) graphite and (b) N-FG.

Figure 6. Schematics of proposed formation mechanism of N-FG.

Figure 7. Quantification of phenolic and hydroxyl groups of AFLG.

Figure 8. Time-dependent UV-vis absorption spectra for the reduction of benzaldehyde catalyzed by (a) AuNCs, (b) N-FG, (c) N-FG-AuNCs hybrid, and (d) AFLG-AuNC hybrid in aqueous media at 25 °C. (e) Structures of benzyl alcohol moiety bearing bioactive molecules.

Table 1: The comparative study of preparation and catalysis applications of nanocomposites. G: graphene, AuNRs: gold nanorods, AuNPs: gold nanoplates, AuNCs: gold nanocrystals, GO: graphene oxide, FRGO: functional reduced graphene oxide, HCNM: hierarchical carbon nanotube membrane, EDA: ethylene diamine, N-PED: N-propyl ethylene diamine, Eq.: Equivalents. [a]purification of products at each stage of FRGO-AuNPs formation.

Figures

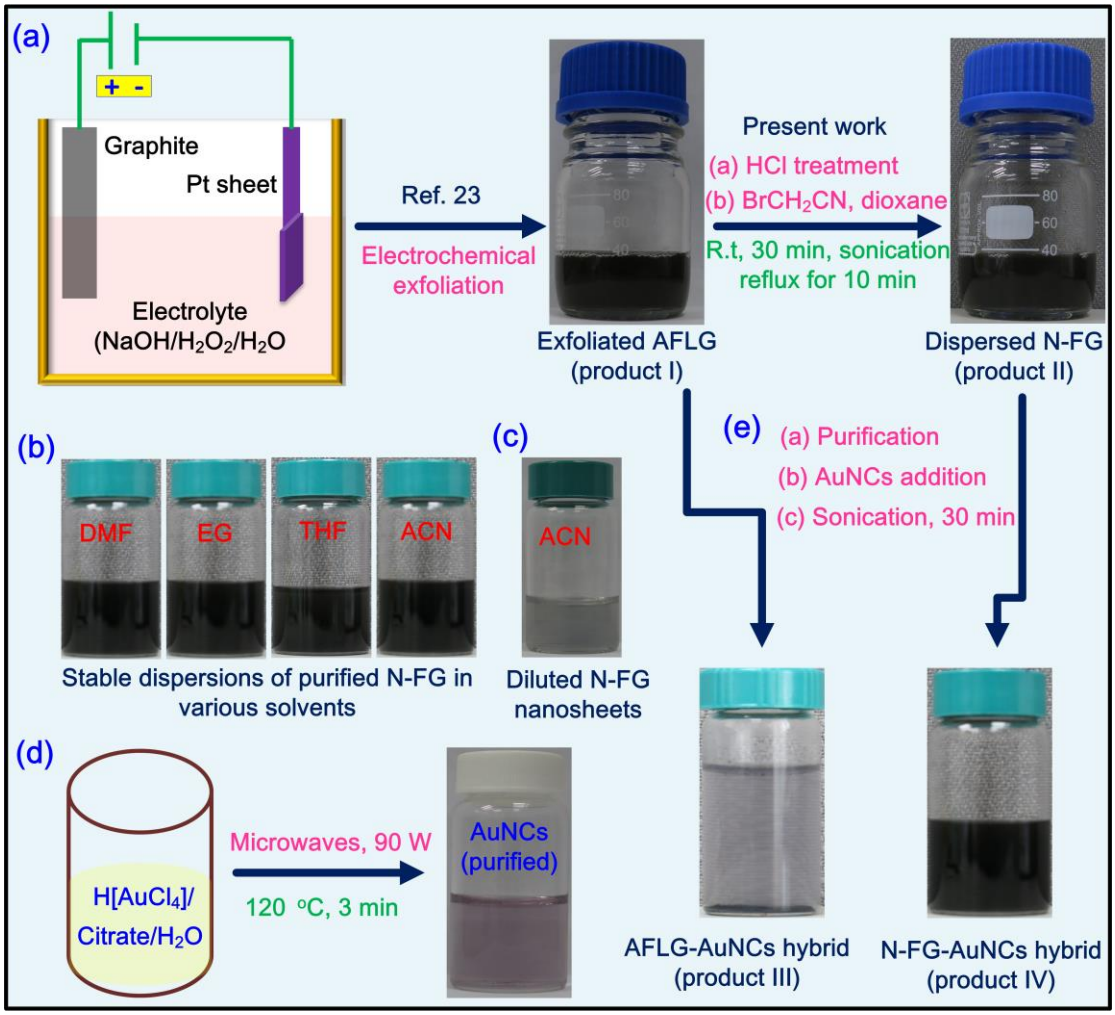

Figure 1

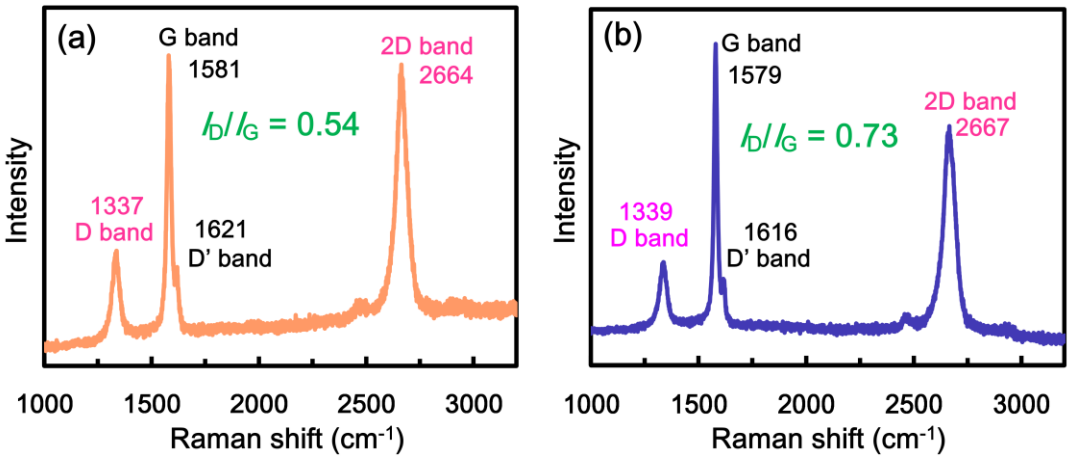

Figure 2

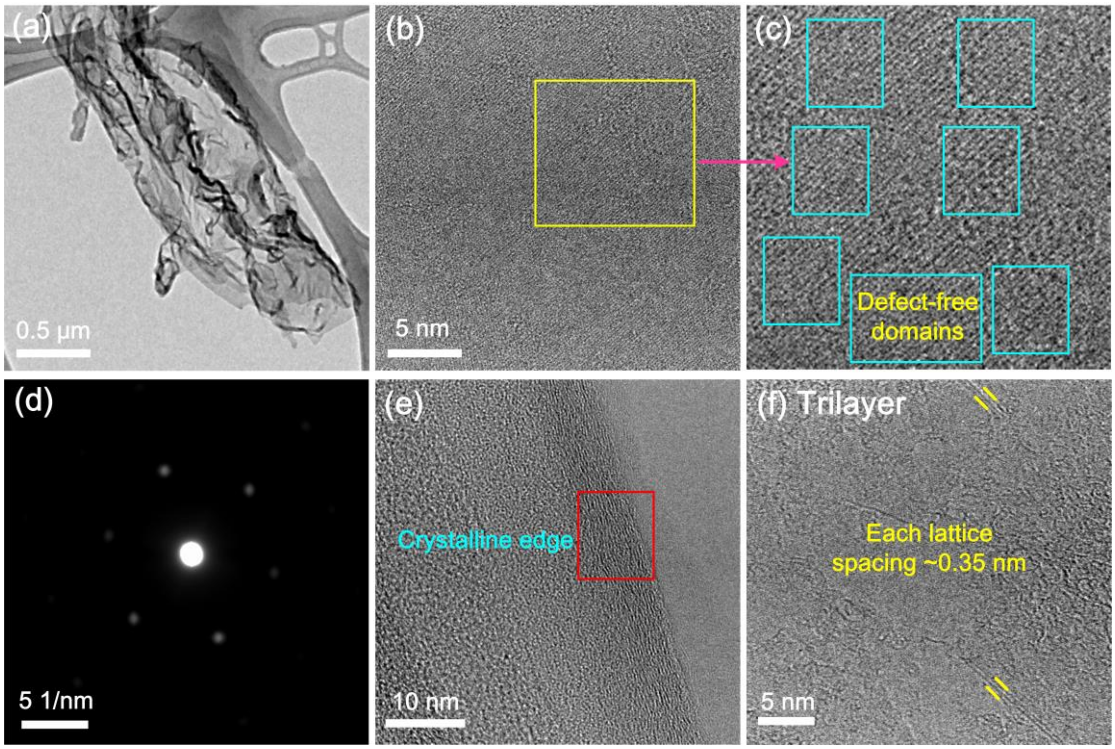

Figure 3

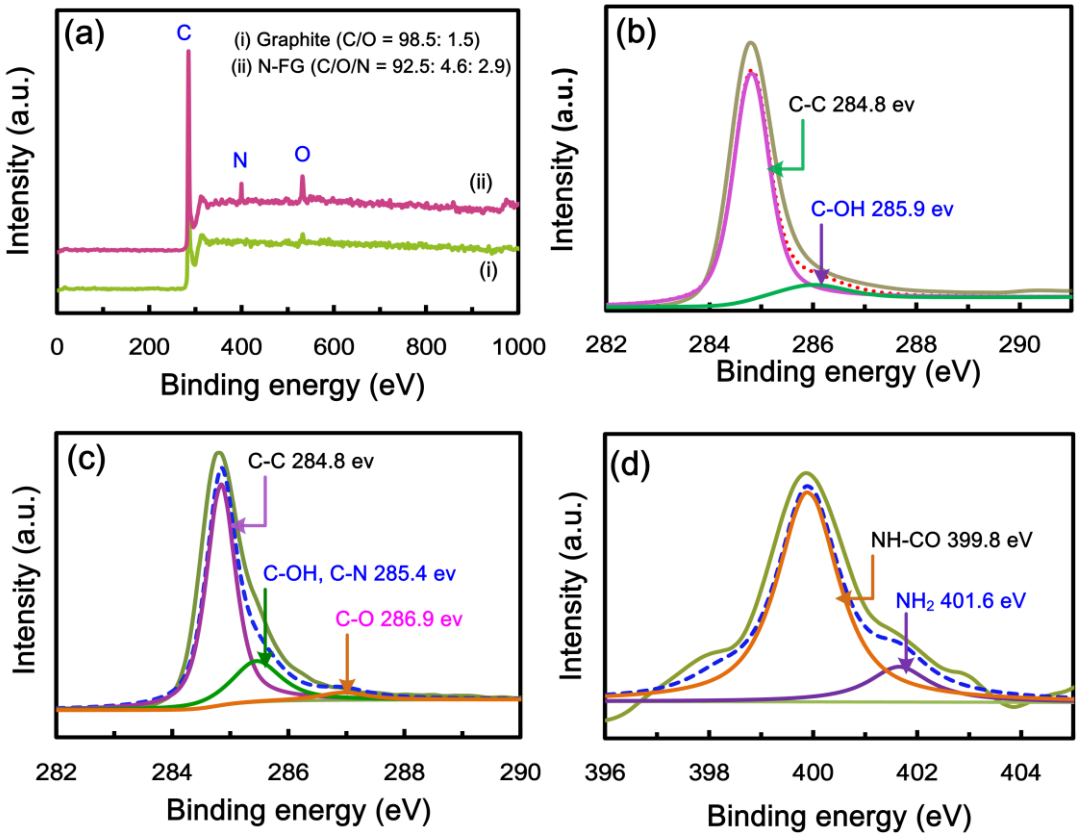

Figure 4

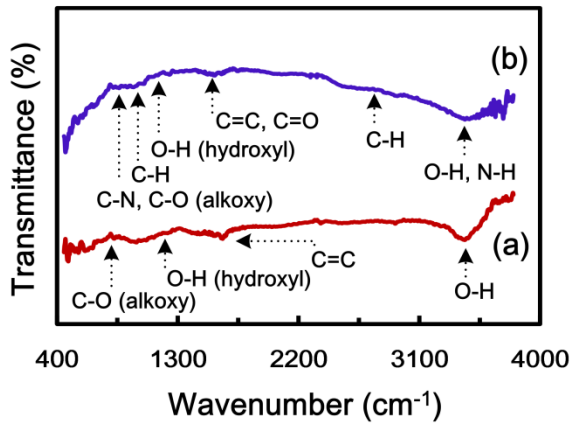

Figure 5

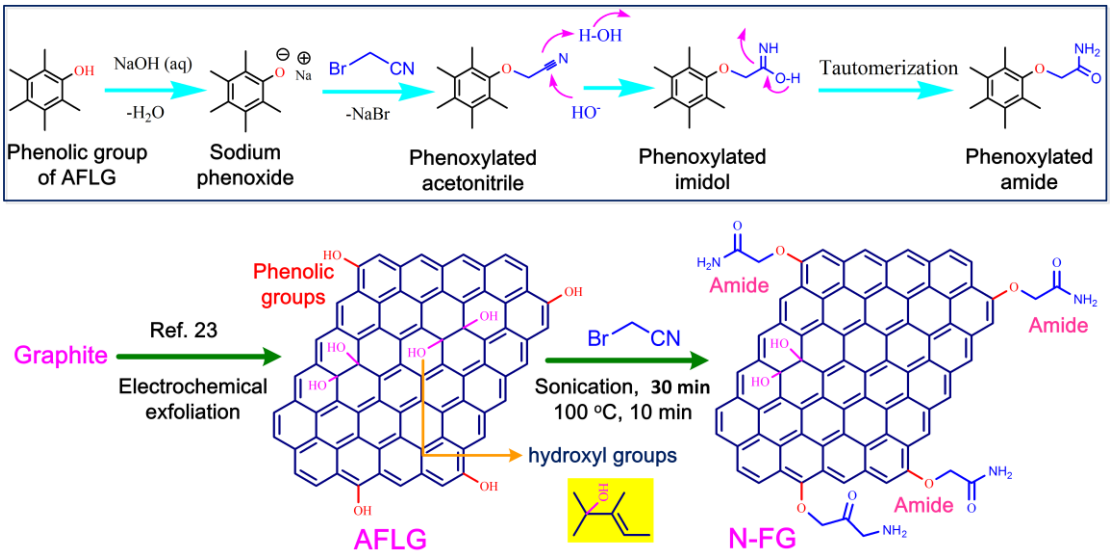

Figure 6

Material	Composition (%) C	O	N	**AFLG oxygen functional groups**
AFLG	94.5	5.5	-	Phenolic groups = 2.9%
N-FG	92.5	4.6	2.9	Hydroxyl groups = 2.6%

Figure 7

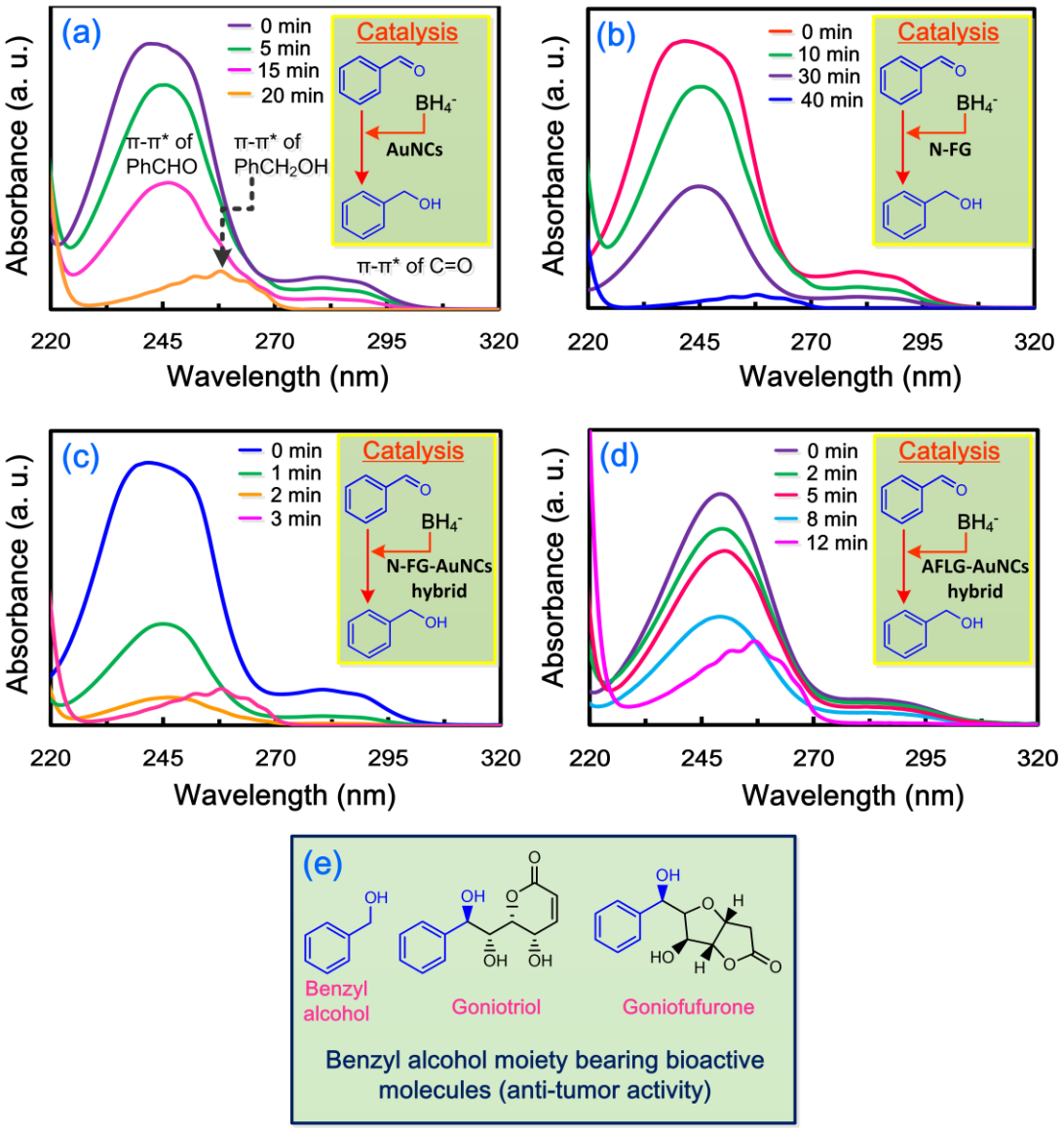
(a)
0 min
5 min
15 min
20 min
π-π* of PhCHO
π-π* of PhCH2OH
π-π* of C=O
Catalysis
BH4-
AuNCs
OH
Absorbance (a. u.)
220 245 270 295 320
Wavelength (nm)
(b)
0 min
10 min
30 min
40 min
Catalysis
BH4-
N-FG
OH
Absorbance (a. u.)
220 245 270 295 320
Wavelength (nm)
(c)
0 min
1 min
2 min
3 min
Catalysis
BH4-
N-FG-AuNCs hybrid
OH
Absorbance (a. u.)
220 245 270 295 320
Wavelength (nm)
(d)
0 min
2 min
5 min
8 min
12 min
Catalysis
BH4-
AFLG-AuNCs hybrid
OH
Absorbance (a. u.)
220 245 270 295 320
Wavelength (nm)
(e)
OH
Benzyl alcohol
OH
O
OH
OH
Goniotriol
OH
HO
H
O
H
O
Goniofufurone
Benzyl alcohol moiety bearing bioactive molecules (anti-tumor activity)

Figure 8

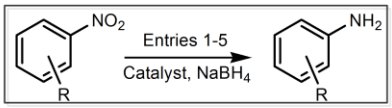

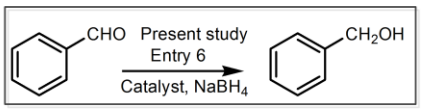

Entry	Catalyst	Preparation method	Precursors & procedure	R	$NaBH_4$ (Eq.)	Time	Ref.
1	G-ZnO-AuNRs	Solution process Hydrothermal	a) Commercial GO b) $Zn(OAc)_2$, EDA, Catechin, GO, AuNCs, H_2O, 90 °C, 1 h c) 300 °C, 2 h	H	- (Photo-catalysis)	140 min	64
2[a]	FRGO-AuNPs	Solution process	a) GO preparation (modified Hummers) b) GO, DMF, N-PED, 80 °C, 10 h, c) Product, DMF, sonication, 30 min, H_2N-NH_2, 90 °C, 24 h (FRGO formed) d) FRGO, DMF, $H[AuCl_4]$, $NaBH_4$, 30 min	*p*-OH	100	15 sec	65
3	GO-AuNCs	Solution process	a) GO preparation (modified Hummers) b) GO, DMAP-AuNCs, rt, 3 h	*p*-OH *o*-NH_2 *p*-NH_2	300	30 min 14 min 40 min	58
4	HCNM-AuNCs	CVD process Solution process	a) 500 °C, 15 min, C_2H_2, H_2, 700 °C, 30 min (HCNM formed) b) PEI, HCNM, 24 h, AuNCs, 12 h	*p*-OH	250	15 min	57
5	RGO-AuNCs	Solution process	a) GO preparation (modified Hummers) b) H_2N-NH_2, H_2O, NH_4OH, 95 °C, 1 h c) RGO, H_2O, AuNCs, rt, 24 h	*o*-NH_2	350	10 sec	66
6	N-FG-AuNCs	Solution process	<u>Present study:</u> Continuous synthesis of N-FG a) Graphite, Aq. 3.0 M NaOH, 130 mM H_2O_2 , 20 min, then 6.0 M HCl, $BrCH_2CN$, Dioxane, sonication, 30 min, 100 °C, 10 min (N-FG formed) b) N-FG, AuNCs, sonication, 30 min	See above entry 6 scheme	3	3 min	-

Table 1